Reduced Order Models for Divergence-Conforming Isogeometric Flow Simulations

T. Kvamsdal[1,2] E. Fonn[2] E. H. van Brummelen[3] A. Rasheed[2]

[1]Department of Mathematical Sciences, NTNU

[2]Applied Mathematics and Cybernetics, SINTEF Digital

[3]Department of Mechanical Engineering, TU/e

Outline

1. Basics of Reduced Basis Methods
2. Stationary Navier-Stokes flow
3. Pressure recovery
4. Numerical examples
5. Results
6. Concluding remarks

Basics of Reduced Basis Methods

Parameter-dependent models

$$\boldsymbol{\mu} \longrightarrow \boxed{\text{Model}} \longrightarrow \boxed{\boldsymbol{u}(\boldsymbol{\mu})}$$

- We are interested generating solutions $\boldsymbol{u}(\boldsymbol{\mu})$ to a physical model that depend on a set of pre-determined *parameters*, $\boldsymbol{\mu} \in \mathcal{P}$.
- Parameters can be: viscosity, heat conductivity, varying boundary conditions, geometry changes, etc.

Parameter-dependent models

Motivation: *many-query* applications. E.g. control systems, optimization, inverse problems and real-time responsiveness.

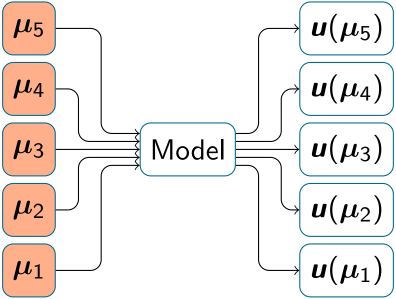

Dimensional reduction

- With conventional (read: FEM, FVM, FDM, and yes, even IGA) methods, this may be impractical if not impossible.
- Too many DoFs N to finish in a realistic timeframe.
- Usually,

$$M = \dim \text{“span”} \left(\{ \boldsymbol{u}(\boldsymbol{\mu}) \,|\, \boldsymbol{\mu} \in \mathcal{P} \} \right) \ll N$$

- Idea: create a model with number of DoFs closely matching the physical dimension of the problem.
- Often, $M \sim 100$ or so!

The vision[1]

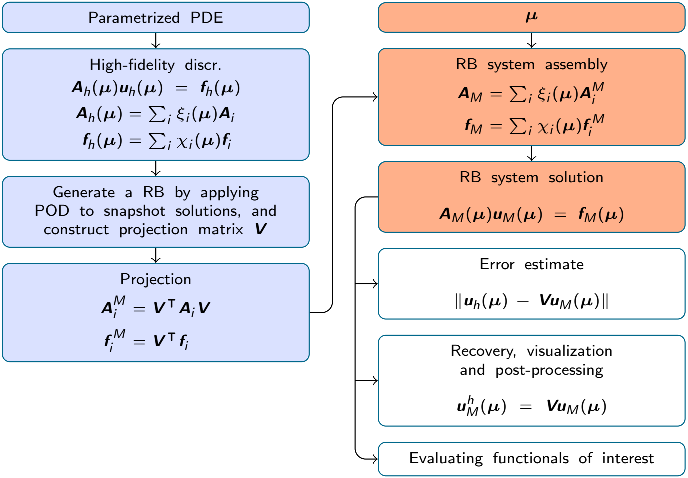

[1] See Quarteroni, Manzoni, and Negri 2016.

Our guiding principle

"**Any**" extra cost in the offline stage is worth paying,
no matter how much, if it makes the online stage faster.

Our guiding principle

All is fair in love, war *and the offline stage*.
— John Lyly (*Euphues*; 1579)

Assembly

- Why the insistence on forms like

$$\boldsymbol{A}_h(\boldsymbol{\mu}) = \sum_i \xi_i(\boldsymbol{\mu})\boldsymbol{A}_i, \qquad \boldsymbol{f}_h(\boldsymbol{\mu}) = \sum_i \chi_i(\boldsymbol{\mu})\boldsymbol{f}_i$$

- Because it makes *assembly* of reduced models fast.
- Each $\boldsymbol{A}_i$ and $\boldsymbol{f}_i$ can be projected independently onto a reduced basis and stored.
- This makes the online stage completely high-fidelity-agnostic.
- Deriving these *affine representations* is the core detail of RBM.

Stationary Navier-Stokes flow

Navier-Stokes equations

$$
\begin{aligned}
-\nu \Delta \boldsymbol{u} + (\boldsymbol{u} \cdot \nabla)\boldsymbol{u} + \nabla p = \boldsymbol{f} &\qquad \text{in } \Omega, \\
\nabla \cdot \boldsymbol{u} = 0 &\qquad \text{in } \Omega, \\
\boldsymbol{u} = \boldsymbol{g} &\qquad \text{on } \Gamma_{\mathrm{D}}, |\Gamma_D| > 0 \\
-p\boldsymbol{n} + \nu(\nabla \boldsymbol{u})\boldsymbol{n} = \boldsymbol{h} &\qquad \text{on } \Gamma_{\mathrm{N}}.
\end{aligned}
$$

Divergence-conforming methods

- Balance between velocity and pressure space is delicate.
- Too many velocity DoFs: poor enforcement of the continuity equation. Too many pressure DoFs: pressure instability.
- A pair of spaces (V, P) is divergence-conforming if $\operatorname{div} V = P$. Ensures the strong (pointwise) form of the continuity equation, and no pressure instabilities.
- IGA unlocks easy construction of such spaces.[2]

[2] Buffa, Sangalli, and Vázquez 2010; Evans and Hughes 2013.

Anatomy of a reduced system

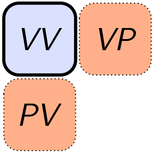

- Usually, the reduced method does not inherit the stability properties of the high-fidelity method.
- Rank-deficient velocity-pressure blocks are common.
- Carefully selecting number of velocity modes and pressure modes seems to help?

$$M_{\mathrm{V}} \approx dM_{\mathrm{P}}$$

Anatomy of a reduced system (cont.)

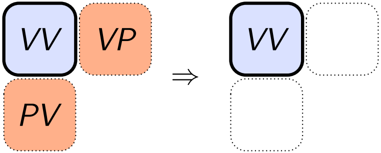

- A divergence-free reduced basis eliminates the coupling, leading to a fully stable velocity-only formulation.
- IGA[3] enables divergence-free high-fidelity solutions,[4] therefore also divergence-free reduced bases.

[3] Hughes, Cottrell, and Bazilevs 2005; Cottrell, Hughes, and Bazilevs 2009.
[4] Evans and Hughes 2013.

Divergence-free basis

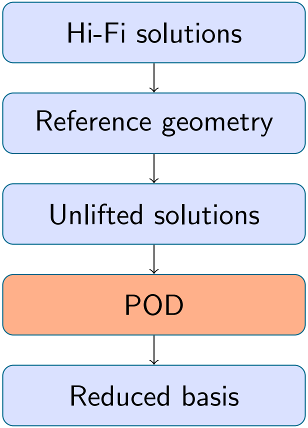

Divergence-free basis

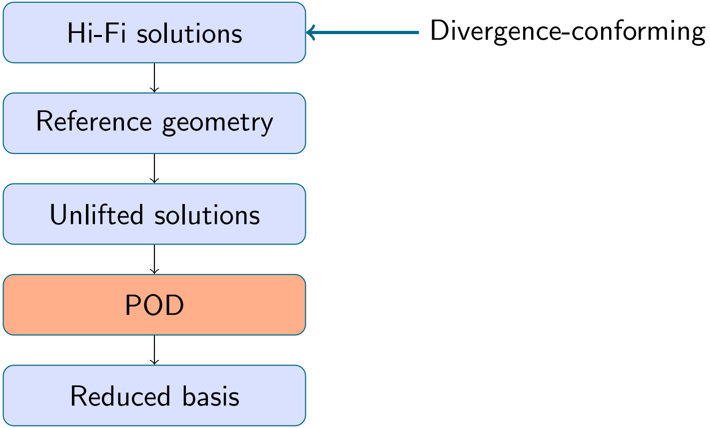

Divergence-free basis

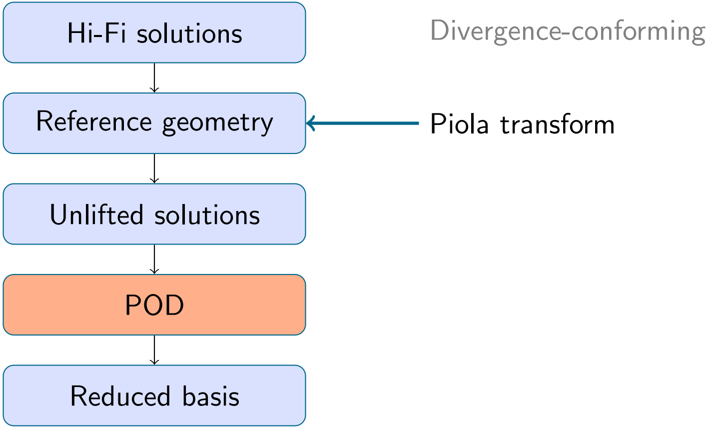

Divergence-free basis

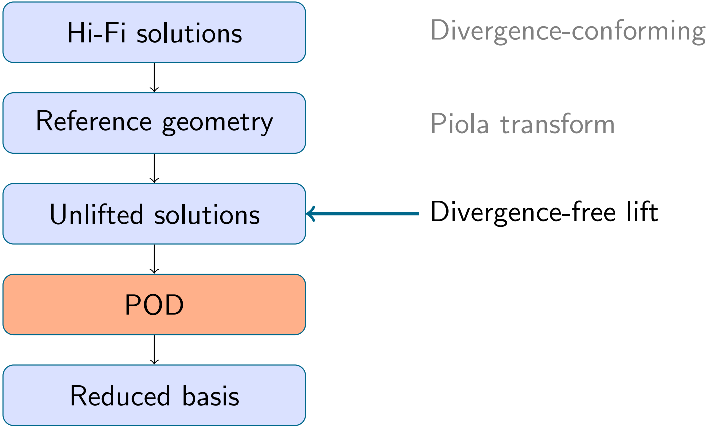

Divergence-free basis

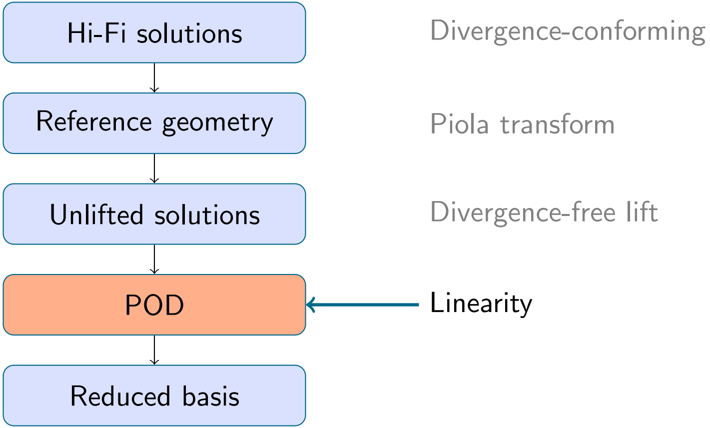

Divergence-free basis

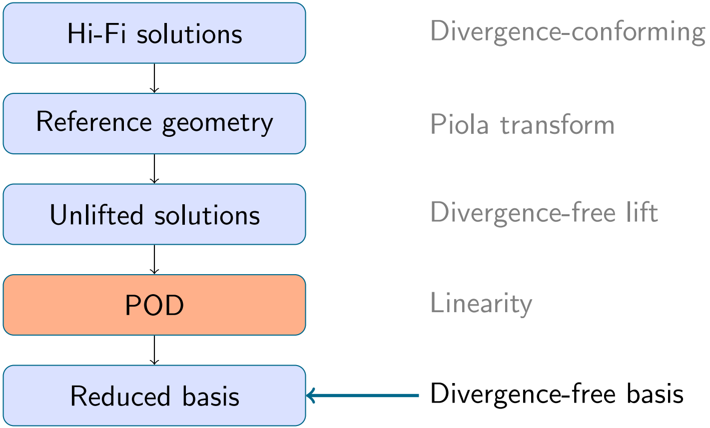

Pressure recovery

Pressure recovery

- The simplest approach is to attach pressure data to divergence-free velocity basis functions.
- Pressure recovery becomes “free” (no linear system to solve, use coefficients from RB velocity solution).
- However, this implies a linear velocity-pressure relationship, in violation of e.g. Navier-Stokes.
- Could work depending on problem.

Pressure recovery

- Another approach is to solve the momentum equation with a different test space.
- The "optimal" test functions are *supremizers*, maximizers of the "sup" part of the inf-sup condition, for any specific pressure solution.
- Supremizers form a reduced space just like velocity and pressure do.
- Supremizers are commonly used to enrich non-divergence-free reduced velocity spaces for stability.[5]

[5] Ballarin et al. 2015.

Anatomy of a reduced system (cont.)

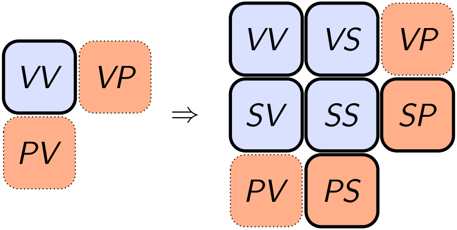

Anatomy of a reduced system (cont.)

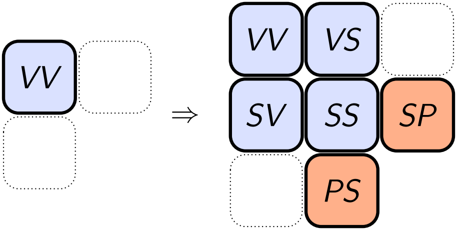

Note the block triangular structure.

Numerical examples

Flow around airfoil

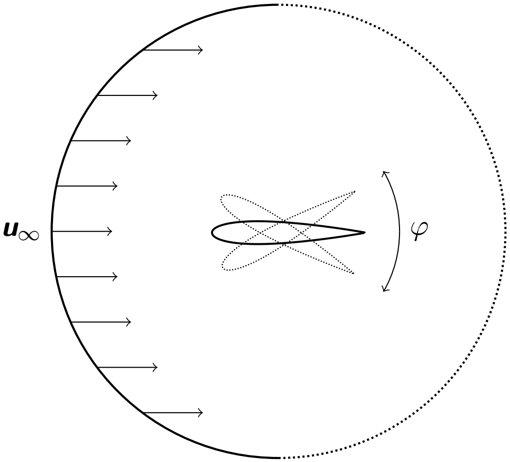

Domain transformation

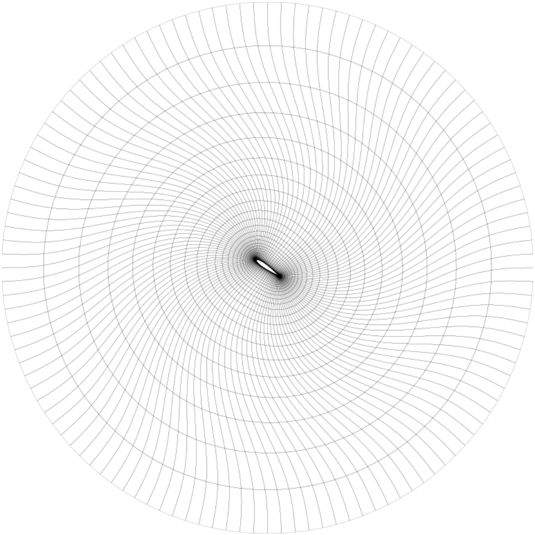

Parameter space

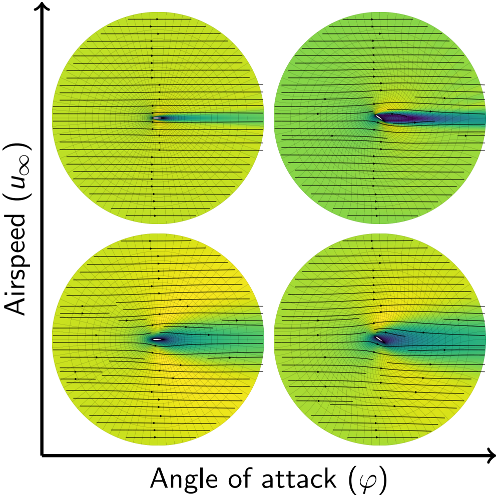

Problem specification

- We will try two high-fidelity methods: a Taylor-Hood (1,2)-method and an IGA (1,2) divergence-conforming method, with both approaches to pressure recovery.
- The parameter domain was chosen as

$$\mathcal{P} = [-35^\circ, +35^\circ] \times [1\,\mathrm{m/s}, 20\,\mathrm{m/s}].$$

- Only *stationary* Navier-Stokes, with $\nu = \frac{1}{6}$.
- We chose equal number of modes in all spaces: $N_\mathrm{V} = N_\mathrm{S} = N_\mathrm{P} = M$.

Affine representations

- Not possible to express the Navier-Stokes problem as finite sums

$$\boldsymbol{A}_h(\boldsymbol{\mu}) = \textstyle\sum_i \xi_i(\boldsymbol{\mu})\boldsymbol{A}_i, \qquad \boldsymbol{f}_h(\boldsymbol{\mu}) = \textstyle\sum_i \chi_i(\boldsymbol{\mu})\boldsymbol{f}_i$$

- Instead, we use truncated polynomial series in φ.[6]
- We can expect about 10 digits of accuracy with a reasonable number of terms ($\sim$25 for TH, $\sim$75 for DC).
- Recall: the intention is to encode *all* parameters explicitly in the representation of the bi- or trilinear forms.

$$\boldsymbol{J} = \sum_i \varphi^i \boldsymbol{B}_i^{(+)} \qquad \boldsymbol{J}^{-\intercal} = \sum_i \varphi_j \boldsymbol{B}_j^{(-)}$$

$$\boldsymbol{J}^{-1}\boldsymbol{J}^{-\intercal} = \boldsymbol{I} + \varphi \boldsymbol{D}_1 - \varphi^2 \boldsymbol{D}_2$$

[6] Fonn et al. 2018.

Affine representations (TH)

$$
\begin{aligned}
(\boldsymbol{\pi}^*_{\boldsymbol{\mu}} a)(\hat{\boldsymbol{u}}, \hat{\boldsymbol{w}}; \varphi) &= \nu \int_{\hat{\Omega}} \nabla \hat{\boldsymbol{u}} : \nabla \hat{\boldsymbol{w}} + \nu\varphi \int_{\hat{\Omega}} \nabla \hat{\boldsymbol{u}} : (\boldsymbol{D}_1 \nabla) \hat{\boldsymbol{w}} \\
&\quad - \nu\varphi^2 \int_{\hat{\Omega}} \nabla \hat{\boldsymbol{u}} : (\boldsymbol{D}_2 \nabla) \hat{\boldsymbol{w}} \\
(\boldsymbol{\pi}^*_{\boldsymbol{\mu}} b)(\hat{p}, \hat{\boldsymbol{w}}; \varphi) &\approx \sum_{i=0}^{2n} \varphi^i \int_{\hat{\Omega}} \hat{p} \boldsymbol{B}_i^{(-)} : \nabla \hat{\boldsymbol{w}} \\
(\boldsymbol{\pi}^*_{\boldsymbol{\mu}} c)(\hat{\boldsymbol{u}}, \hat{\boldsymbol{v}}, \hat{\boldsymbol{w}}; \varphi) &\approx \sum_{i=0}^{2n} \varphi^i \int_{\hat{\Omega}} (\hat{\boldsymbol{u}} \cdot \boldsymbol{B}_i^{(-)} \nabla) \hat{\boldsymbol{v}} \cdot \hat{\boldsymbol{w}}
\end{aligned}
$$

Affine representations (IGA)

$$
\begin{aligned}
(\boldsymbol{\pi}^*_{\boldsymbol{\mu}} a)(\hat{\boldsymbol{u}}, \hat{\boldsymbol{w}}; \varphi) &= \nu \sum_{i,j=0}^{2n} \varphi^{i+j} \int_{\hat{\Omega}} \nabla(\boldsymbol{B}_i^{(+)} \hat{\boldsymbol{u}}) : \nabla(\boldsymbol{B}_j^{(+)} \hat{\boldsymbol{w}}) \\
&\quad + \nu \sum_{i,j=0}^{2n} \varphi^{i+j+1} \int_{\hat{\Omega}} \nabla(\boldsymbol{B}_i^{(+)} \hat{\boldsymbol{u}}) : (\boldsymbol{D}_1 \nabla)(\boldsymbol{B}_j^{(+)} \hat{\boldsymbol{w}}) \\
&\quad - \nu \sum_{i,j=0}^{2n} \varphi^{i+j+2} \int_{\hat{\Omega}} \nabla(\boldsymbol{B}_i^{(+)} \hat{\boldsymbol{u}}) : (\boldsymbol{D}_2 \nabla)(\boldsymbol{B}_j^{(+)} \hat{\boldsymbol{w}}) \\
(\boldsymbol{\pi}^*_{\boldsymbol{\mu}} b)(\hat{p}, \hat{\boldsymbol{w}}; \varphi) &= \sum_{i,j=0}^{2n} \varphi^{i+j} \int_{\hat{\Omega}} \hat{p} \boldsymbol{B}_i^{(-)} : \nabla \left(\boldsymbol{B}_j^{(+)} \hat{\boldsymbol{w}} \right) \\
(\boldsymbol{\pi}^*_{\boldsymbol{\mu}} c)(\hat{\boldsymbol{u}}, \hat{\boldsymbol{v}}, \hat{\boldsymbol{w}}; \varphi) &= \sum_{i,j=0}^{2n} \varphi^{i+j} \int_{\hat{\Omega}} (\hat{\boldsymbol{u}} \cdot \nabla) \boldsymbol{B}_i^{(+)} \hat{\boldsymbol{v}} \cdot \boldsymbol{B}_j^{(+)} \hat{\boldsymbol{w}}.
\end{aligned}
$$

Results

Spectrum

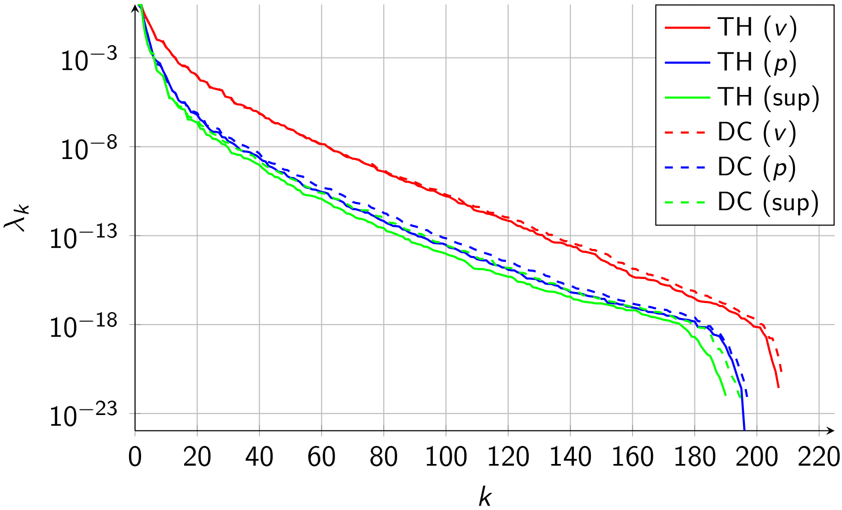

10^{-3}
10^{-8}
10^{-13}
10^{-18}
10^{-23}
λ_k
0
20
40
60
80
100
120
140
160
180
200
220
k
TH (v)
TH (p)
TH (sup)
DC (v)
DC (p)
DC (sup)

Basis functions (v, TH, 1)

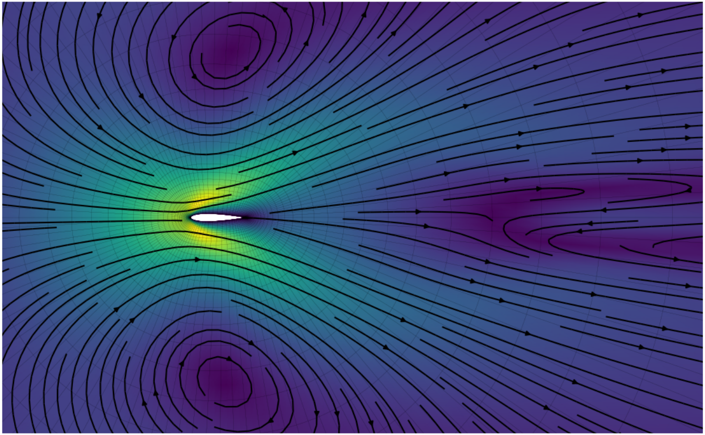

Basis functions (v, TH, 2)

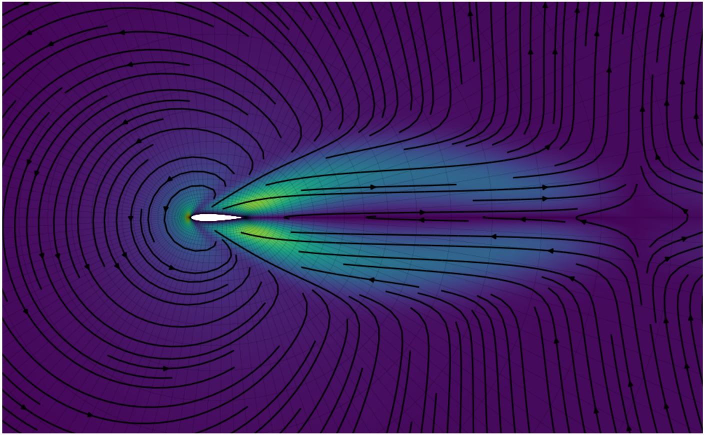

Basis functions (v, TH, 3)

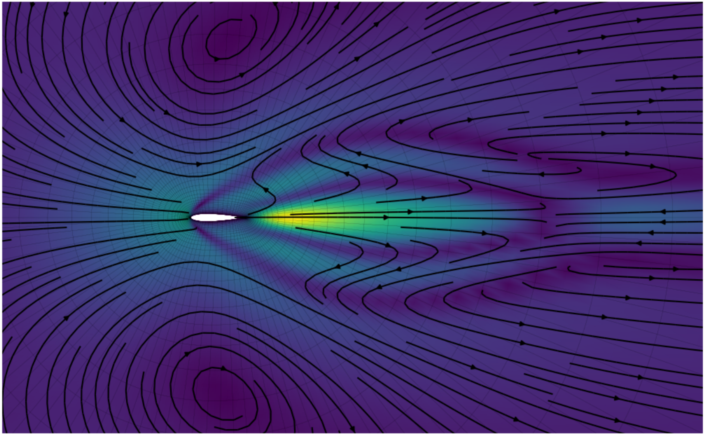

Basis functions (v, TH, 4)

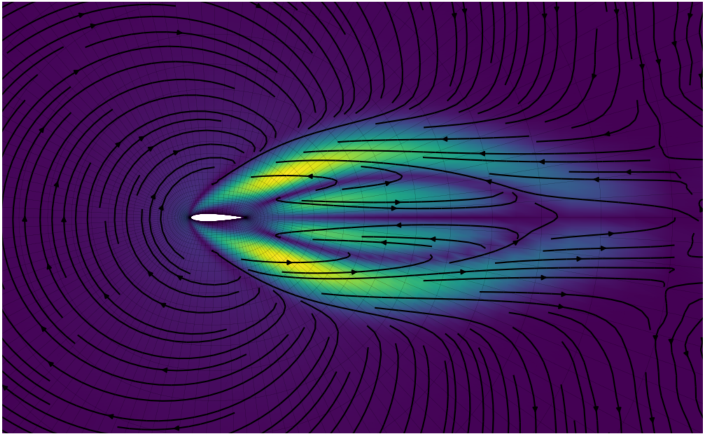

Basis functions (v, DC, 1)

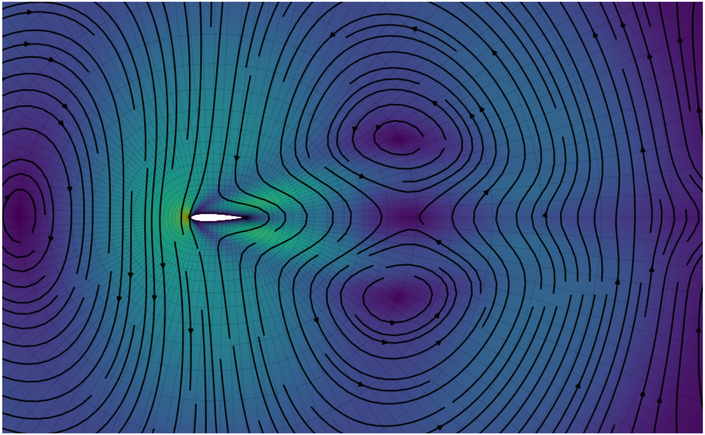

Basis functions (v, DC, 2)

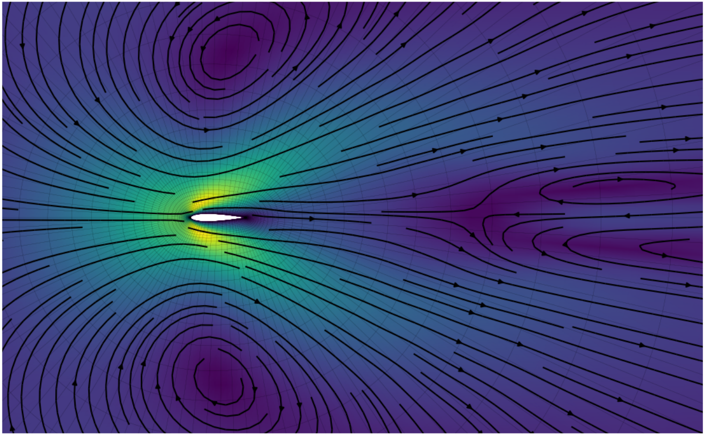

Basis functions (v, DC, 3)

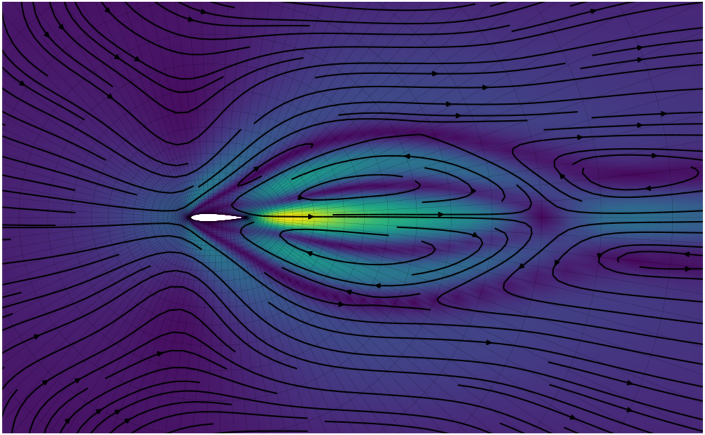

Basis functions (v, DC, 4)

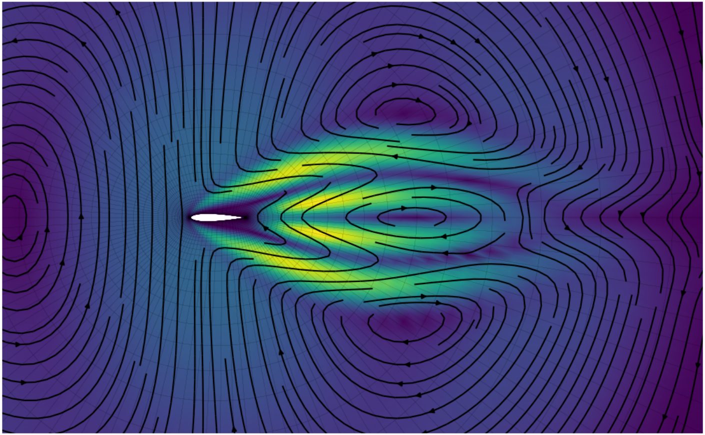

Convergence

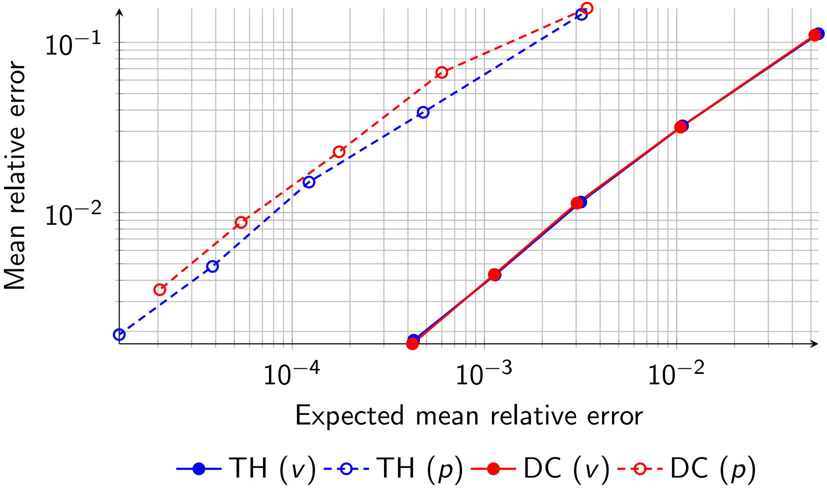

Convergence

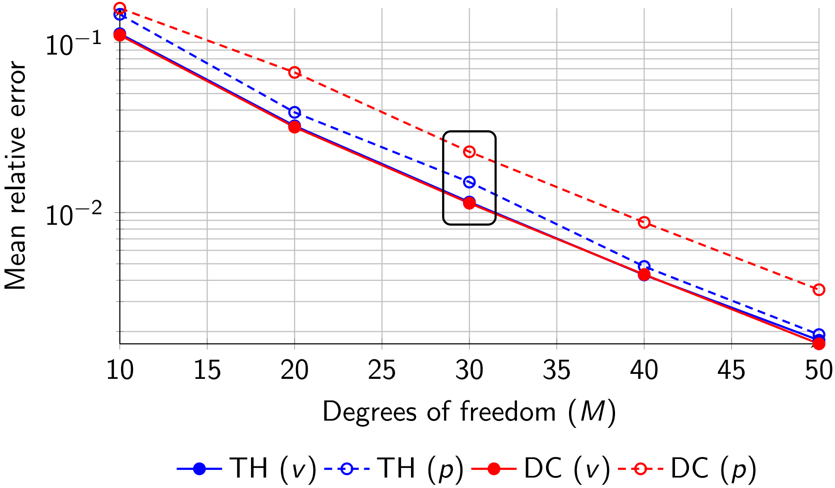

Convergence

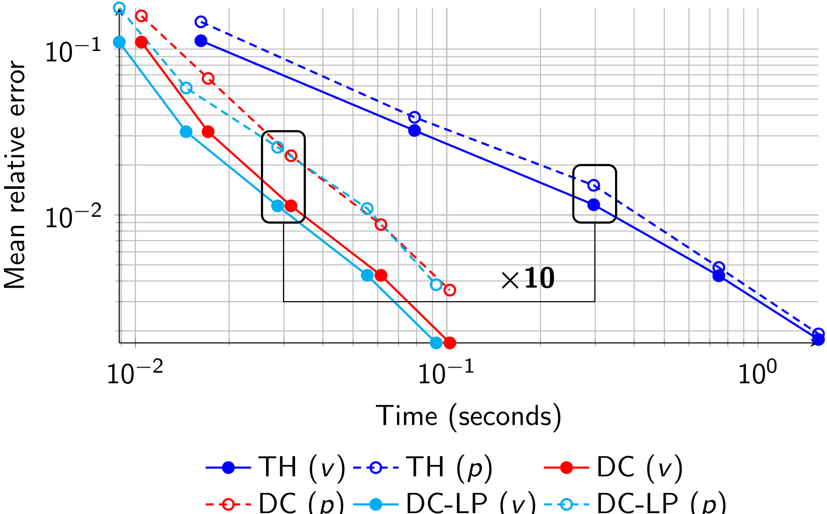

Speedup factors

$\sharp$ DoFs (M)	**Taylor-Hood**	**Conforming**
10	1483	6890
20	390	2616
30	111	1441
40	52	843
50	27	502

Summary

- Reduced order models offer dramatic speed-ups for certain applications.
- They combine nicely with IGA and div-compatible spaces to form fully divergence-free function spaces without need for pressure fields.
- Divergence-free RBMs can be much faster than other RBMs, in spite of additional complexity in the offline stage (remember, all is fair there.)

Thank you!

References

Ballarin, Francesco et al. (2015). “Supremizer stabilization of POD-Galerkin approximation of parametrized steady incompressible Navier-Stokes equations”. In: *International Journal for Numerical Methods in Engineering* 102.5, pp. 1136–1161. ISSN: 1097-0207. DOI: 10.1002/nme.4772. URL: http://dx.doi.org/10.1002/nme.4772.

Buffa, Annalisa, Giancarlo Sangalli, and Rafael Vázquez (2010). “Isogeometric analysis in electromagnetics: B-splines approximation”. In: *Computer Methods in Applied Mechanics and Engineering* 199.17-20, pp. 1143–1152.

Cottrell, J Austin, Thomas R J Hughes, and Yuri Bazilevs (2009). *Isogeometric Analysis: Toward Integration of CAD and FEA*. Wiley.

Evans, John A. and Thomas J R Hughes (2013). “Isogeometric divergence-conforming B-splines for the steady Navier-Stokes equations”. In: *Mathematical Models and Methods in Applied Sciences* 23.8, pp. 1421–1478. ISSN: 0218-2025. DOI: 10.1142/S0218202513500139.

Fonn, E. et al. (2018). “Fast divergence-conforming reduced basis methods for steady Navier-Stokes flow”. Submitted.

Hughes, Thomas JR, John A Cottrell, and Yuri Bazilevs (2005). “Isogeometric analysis: CAD, finite elements, NURBS, exact geometry and mesh refinement”. In: *Computer methods in applied mechanics and engineering* 194.39, pp. 4135–4195.

Quarteroni, Alfio, Andrea Manzoni, and Federico Negri (2016). *Reduced basis methods for partial differential equations*. Springer International Publishing.